Asian Journal of Chemistry; Vol. 26, No. 20 (2014), 7055-7060

ASIAN JOURNAL OF CHEMISTRY

http://dx.doi.org/10.14233/ajchem.2014.17876

Facile Synthesis, Characterization and Visible-Light Photocatalytic Performance of Ag_3PO_4

LI LIN[1,2], MANHONG HUANG[1,*], LIPING LONG[2], ZHE SUN[1] and DONGHUI CHEN[1,3,*]

[1]School of Environmental Science and Engineering, Donghua University, Shanghai 201620, P.R. China
[2]School of Chemical and Environmental Engineering, Hunan City University, Yiyang 413000, P.R. China
[3]Shanghai Institute of Technology, Shanghai 200235, P.R. China

*Corresponding authors: E-mail: linlilejin@126.com; huangmanhong@dhu.edu.cn

Received: 23 April 2014; *Accepted*: 27 June 2014; *Published online*: 25 September 2014; AJC-16066

Silver(I) phosphate (Ag_3PO_4) photocatalysts were synthesized *via* a facile solid phase ion-exchange method, X-ray diffraction, scanning electron microscopy and UV-visible diffuse reflectance spectroscopy (DRS) were used to characterize the as-prepared samples. The photocatalytic performance and mechanism of as-prepared samples were investigated by the degradation of tetracyclines in aqueous solution under visible light irradiation ($\lambda > 420$ nm). The results indicated that the as-prepared samples were irregular spherical morphology with paticle size of 0.5-1.5 μm and exibited strong light absorbance in the visible light region. The superior photocatalytic activity and removal efficiency of total organic carbon (TOC) were also observed. The mechanism expriment results demonstrated that the $O_2^{\bullet-}$, $^{\bullet}OH$ and hole were all reactive oxygen species and the possible photocatalytic mechanism was proposed.

Keywords: Ag_3PO_4, Photocatalyst, Tetracycline, Visible light.

INTRODUCTION

To solve the environmental pollution and energy shortage, the heterogeneous photocatalytic technique by titanium dioxide (TiO_2) has been considered as an environmentally friendly technique for the elimination of organic contaminants and has attracted much attention over the past 30 years[1-3]. However, owing to its wide bandgap (3.2 eV), TiO_2 can only be activated by UV light irradiation (accounting for just 4 % of solar irradiation) which hinders the practical application of TiO_2. To exploit new effective visible-light-driven photocatalysts, various kinds of semiconductor materials, such as C-N-S tridoped[4-6] TiO_2, TiO_2/BiOI and AgI/BiOI composites, have been developed as photocatalysts which can respond to both UV and visible light.

Recently, silver(I) phosphate (Ag_3PO_4) has been found to possess excellent photocatalytic ability under visible-light irradiation for O_2 evolution from water, due to the high-efficient separation of photoexcited electrons and holes[7]. Bi *et al.*[8] have revealed a facet effect on the photocatalytic performance of single-crystalline Ag_3PO_4 for decolorization of organic dyes. Ming *et al.*[9] have observed sunlight-induced photodegra-dation of rhodamine B by Ag_3PO_4. The photodegra-dation rate of methylene blue *via* Ag_3PO_4 has been found far beyond that of other visible-light-driven photocatalysts such as $BiVO_4$ and commercial TiO_2-xNx[10,11]. However, the application researches on the Ag_3PO_4 photocatalytst under visible-light irradiation have been focused on dyes degradation, other organic contaminants such as antibiotics have received few attention. Furthermore, the mechanism of Ag_3PO_4 photocatalytic degradation under visible light and the reactive oxygen species involved in photocatalytic reaction has remained unclear to date.

In this study, a facile solid phase ion-exchange reaction was developed to synthesize Ag_3PO_4 at room temperature. Tetracycline residues, as one kind of pseudo-persistent pollutant, have become one of the most concerned issues due to their potential adverse effects on human beings and the aquatic ecological environment[4]. Therefore, tetracycline was selected as representative pollutant targets to evaluated the photocatalytic performance of as-prepared samples under visiblelight irradiation ($\lambda > 420$ nm). Moreover, the possible photocatalysis mechanism based on radical trapping experiments and fluorescence technique was also investigated.

EXPERIMENTAL

Synthesis of Ag_3PO_4 photocatalyst: Silver(I) phosphate powder samples were prepared by the simple solid phase ion-exchange method: 3.58 g of $Na_2HPO_4 \cdot 12H_2O$ and 1.70 g of $AgNO_3$ were thoroughly mixed in an agate mortar and ground until the initially white color changed to yellow. The mixture was then washed with distilled water several times in order to remove any unreacted raw material and the produced $NaNO_3$.

Finally, the vivid yellowish powders obtained were dried at 70 °C overnight in the dark.

Characterization of Ag_3PO_4 photocatalyst: The as-obtained Ag_3PO_4 powder samples were characterized by X-ray diffraction patterns using a Rigaku D/max-2550 diffractometer, using filtered CuK_α radiation operationg at an accelerating voltage of 40 kV and current of 200 mA. The sample was scanned at 2θ from 5 to 90 °. The morphology and size of the as-prepared Ag_3PO_4 product were characterized by scanning electron microscopy (FEI Quanta-250). UV-visible diffuse reflectance spectras were acquired *via* a Perkin Elmer Lambda 35 spectrophotometer, using $BaSO_4$ as the reference.

Photocatalytic evaluation of Ag_3PO_4 photocatalyst: The photocatalytic experiments were carried out in a photochemical reactor (XPA-VII, Nanjing Xujiang Machineelectronic Plant, China), equipped with 500 W Xe lamp combined with a 420 nm cut-off filter as the light source. All photocatalytic reactions were performed using the same initial conditions: 100 mL of tetracycline solution (20 mg/L) was mixed with 100 mg catalyst under constant magnetic stirring. Before irradiation, the suspension was stirred for 20 min in the dark to reach adsorption-desorption equilibrium. At given time intervals, approximately 2.5 mL of the suspension was timely taken out and the solids were subsequently removed from the solution through centrifugation (10000 rpm, 10 min). Throughout the reaction, the concentration of tetracycline in the solution was determined by UV-visible spectroscopy (UV-3010, Shimadzu, Japan, λ = 367 nm). Total organic carbon was measured on a Shimadzu TOC-VCPH analyzer.

Terephthalic acid could be employed as a probe molecule to detect the produced hydroxyl radicals[12]. The fluorescence intensity around 425 nm, can be ascribed to the characteristic of 2-hydroxyterephthalic acid, is proportional to the amount of hydroxyl radicals formed in solution[13,14]. To detect the •OH radicals, 0.05 g of as prepared Ag_3PO_4 was dispersed in a 50 mL of terephthalic acid solution, the concentration of terephthalic acid was set at 5×10^{-4} M in 2×10^{-3} M NaOH solution. Given 20 min intervals, the suspension solution was sampled, centrifuged and measured on a Shimadzu RF5301 type fluorescence spectrophotometer. The excitation wavelength used was 315 nm.

RESULTS AND DISCUSSION

XRD analysis: Fig. 1a shows XRD patterns of as-prepared Ag_3PO_4 sample by the simple ion-exchange method. The main characteristic diffraction peaks at 21.03, 29.84, 33.44, 36.72, 42.60, 47.92, 52.82, 55.14, 57.41, 61.77 and 65.96º were indexed to the (110), (200), (210), (211), (220), (310), (222), (320), (321), (400) and (330) planes of the cubic Ag_3PO_4 phase, respectively. All patterns match with the JPCDS (74-1876) standard data of Ag_3PO_4 very well. In addition, the as-prepared Ag_3PO_4 exhibited strong and sharp diffraction peaks which revealed well crystalline nature of Ag_3PO_4. Fig. 1b shows XRD patterns of cycling Ag_3PO_4 sample for the first time. Compared with the initial sample, some new diffraction peaks at 38.22, 44.42, 64.58 and 77.50º appeared. The four diffraction peaks match respectively with the (111), (200), (220) and (311) crystalline planes of metallic Ag (JCPDS file: 65-2871), which

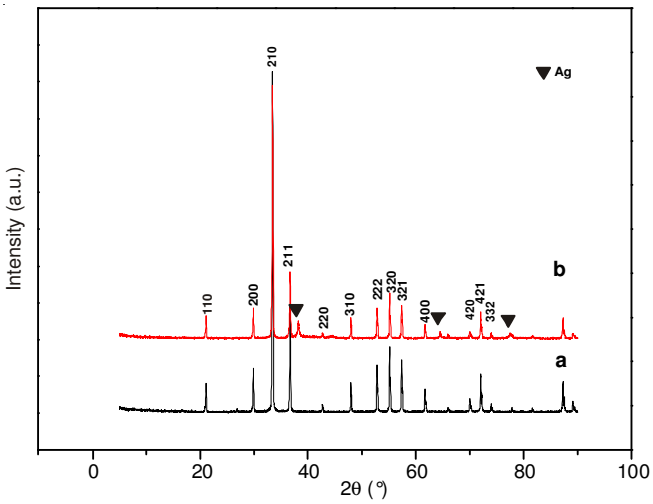

Fig. 1. XRD patterns of the Ag_3PO_4 powders (a) and the cycling Ag_3PO_4 (b)

were marked with "▼" , no other peaks of impurities or other phases such as Ag_xO were observed in XRD patterns. These results indicated that metallic Ag had produced under visible light irradiation. The suspension became black after the Xe lamp turned on could also confirm the change.

SEM analysis: Fig. 2 shows the typical SEM images of the as-synthesized Ag_3PO_4 photocatalyst with different magnifications. From the magnified views of Fig. 2, Ag_3PO_4 particles exhibited irregular morphology with non-uniform diameters. The particles with different particle size gathered to form large agglomerates through physical attraction. The particle size of the crystals was estimated to be about 0.5-1.5 μm.

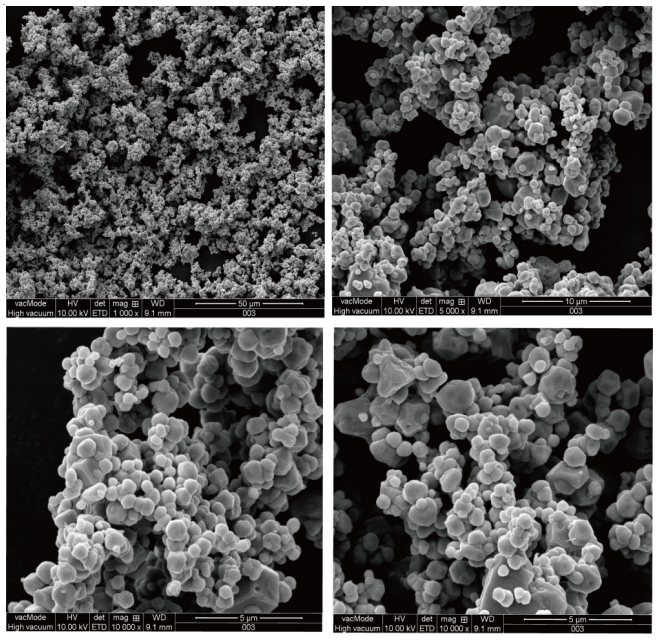

Fig. 2. SEM images of the Ag_3PO_4 sample

UV-visible analysis: The optical properties of as-synthesized Ag_3PO_4 photocatalyst were also investigated. As shown in Fig. 3, the shape of ultraviolet-visible diffuse reflectance spectrum was consistent with the previous report[7] which showed the strong photoabsorption in UV and visible region, the absorption edge was at approximately 530 nm. The band gap

energy of as-synthesized samples could be calculated by the following formula[15] eqn. 1:

$$\alpha h\nu = A(h\nu - E_g)^{n/2} \quad (1)$$

where α, hν, A and E_g are optical absorption coefficient, the photonic energy, proportionality constant and bandgap, respectively. n depends on the characteristics of the transition in a semiconductor, including direct transitions (n = 1) or indirect transitions (n = 4). The band gap energy could be estimated from a plot of $(\alpha h\nu)^{1/2}$ *vs*. the photon energy (hν). The x-axis intercept of the tangent to the plot approached the band gap energy of the sample (Fig. 3). The estimated indirect band gap of Ag_3PO_4 is 2.26 eV, as well as, direct transition is 2.36 eV. This result indicated that the as-prepared samples could be activated by visible light which is similar to previous reports[7,8].

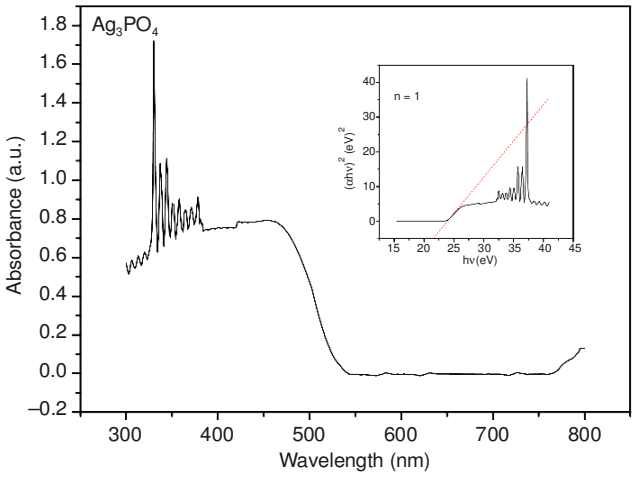

Fig. 3. UV-visible diffuse reflectance spectra of the Ag_3PO_4 powders

Additionally, the valence band (VB) and conduction band (CB) edge potentials of as-synthesized Ag_3PO_4 were estimated *via* Mulliken electronegativity theory[16-18]: $E_{VB} = X - E^e + 0.5\ E_g$; $E_{CB} = E_{VB} - E_g$, where E_{VB} is the valence band edge potential, X is the electronegativity of the semiconductor, which is the geometric mean of the electronegativity of the constituent atoms, E^e standard electrode potential on the hydrogen scale (4.5 eV) and E_g is the band gap energy of the semiconductor. The calculated valence band edge potential results were 2.59 eV (indirect band gap) and 2.65 eV (direct band gap), On the other hand, the calculated conduction band edge potential results were +0.33 eV (indirect band gap) and +0.27 eV (direct band gap).

Evaluation of photocatalytic activity: The photocatalytic performance of the as synthesized Ag_3PO_4 product was evaluated by degradation of tetracyclines under visible light irradiation (λ = 420 nm) with a Xe lamp of 500 W. On the basis of the previous literatures[19-21], BiOBr was reported to possess higher visible-light-photocatalytic activity than P_{25}-TiO_2. According to the literature[19], the BiOBr samples were synthesized for comparison, the photocatalytic activities of the BiOBr was investigated under the identical experimental conditions. The results were illustrated in Fig. 4. The photolysis of tetracyclines upon visible-light irradiation was almost negligible. About 3 % of the tetracyclines in solution was

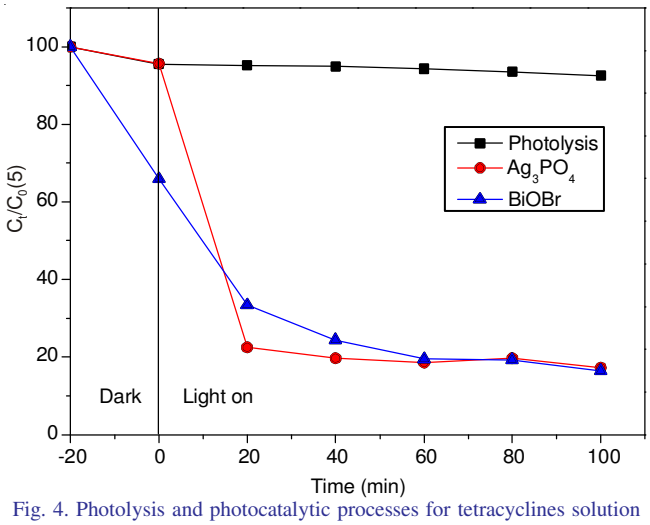

Fig. 4. Photolysis and photocatalytic processes for tetracyclines solution

adsorbed by Ag_3PO_4 in the dark for 20 min. When the light turned on, the degradation of tetracyclines progressed rapidly and 78 % of tetracyclines was photodegraded within 20 min. On the contrary, only 67 % of tetracyclines was removed by BiOBr and about 34 % of tetracyclines was adsorbed among this removal rate. The superior visible light photocatalytic activity of as-prepared Ag_3PO_4 may arises from the surface plasmon resonance of deoxidized Ag nanoparticles and the inductive effect of PO_4^{3-} help e^-/h^+ separation of the high efficiency[22-24]. However, the photodegradation percentage increased slowly with the increasing of time. The same phenomenon was observed over the BiOBr photocatalyst. We deduced that no enough tetracyclines molecules were adsorpted and then reacted with the active species may be the major reason for the low photodegradation ratio in later stage.

To further investigate the mineralization efficiency of tetracyclines, the removal efficiency of total organic carbon (TOC) was also evaluated and the results were shown in Fig. 5. The removal percentage of tetracyclines had reached 40.4 % whithin 270 min, indicating the mineralization of tetracyclines over Ag_3PO_4 under visible light irradiation. Compared to tetracyclines degradation, the slower removal rate of TOC ascribed to many intermediate products produced at first during the photocatalytic reaction process and then gradually mineralized[25,26].

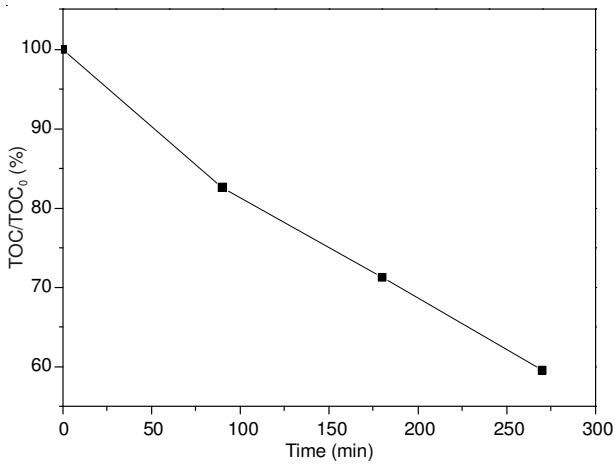

Fig. 5. Change of total organic carbon with irradiation time under visible light irradiation

Effect of pH value: The pH value is usually regarded as one of the most important factors for photocatalytic process. To elucidate the effect of pH on the photodegradation of tetracyclines, pH values were adjusted to 2, 6.9 and 11 by HNO_3 and NH_4OH, respectively. The photodegradation results were shown in Fig. 6, it can be seen that the photodegradation of tetracyclines was significantly restrained in alkali condition, but a little declined in the acid solution. Generally, the alkali condition is beneficial for the generation of hydroxyl radicals which is the major reactive oxygen species in photocatalytic process, the experimental results demonstrated that hydroxyl radicals may not generate *via* the photogenerated hole reacting with OH ions. Additionally, the dissolution of Ag_3PO_4 in the acid and alkali solution decreased the tetracyclines degradation. Therefore, it can be concluded the best pH condition was in the neutral condition.

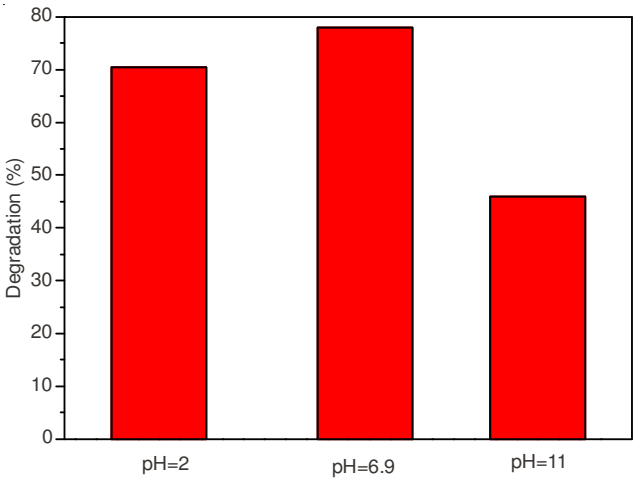

Fig. 6. Effect of tetracyclines degradation at different pH value

Photocatalyst stability: To investigate the photocatalytic reusability of Ag_3PO_4, the repeatability experiments of as-prepared samples were performed under the same conditions. Although a little decreasing of the photocatalytic ability (Fig. 7), the photocatalytic activity of Ag_3PO_4 did not exhibit significant loss after three recycling runs. So, Ag_3PO_4 had favorable reusability under visible light.

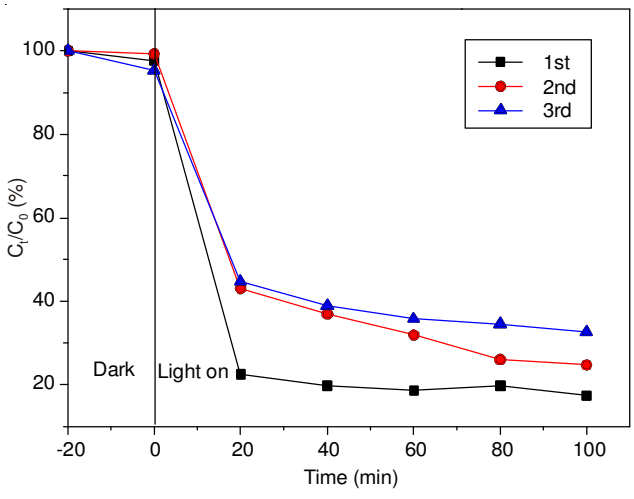

Fig. 7. Recycling tests of photocatalytic degradation of tetracyclines by Ag_3PO_4 catalyst

Photocatalytic mechanism: To further investigate the photocatalytic mechanism of Ag_3PO_4, the reactive oxygen species trapping experiments were performed by using three different radicals scavenger under visible light. It is well-known that $^{\bullet}OH$, $O_2^{\bullet-}$ and h^+ have been implicated as predominant reactive oxygen species in photocatalytic oxidation reactions. Thus, 1 M isopropyl alcohol (IPA), ammonium oxalate (AO) and benzoquinone (BQ) were added to the reaction solution as $^{\bullet}OH$, hole and $O_2^{\bullet-}$ radical scavengers respectively[22,23]. From Fig. 8, it is clear that the addition of IPA and AO slightly inhibited the degradation rate of tetracyclines by Ag_3PO_4 compared with no scavenger. This result indicated that the $OH^{\bullet}$ radicals and photoinduced holes were the active oxygen species in this photocatalytic process. But the calculated valence band potential of Ag_3PO_4 (+2.65 V *vs.* NHE) was less positive than the standard oxidation potential of $^{\bullet}OH$ [$E°(^{\bullet}OH/H_2O)$ = +2.68 V *vs.* NHE], indicating that the E_{VB} on the Ag_3PO_4 surface was insufficient to oxidize the adsorbed H_2O to $^{\bullet}OH$[7,27]. So, the $^{\bullet}OH$ radicals may be formed through other routes. Interestingly, the photocatalytic degradation of tetracyclines was significantly suppressed by the adding of benzoquinone (BQ) which illustrated that $O_2^{\bullet-}$ radicals played a critical role in the tetracyclines degradation in Ag_3PO_4 suspension under visible light. However, $E°(O_2/O_2^{\bullet-})$ (+0.13 eV *vs.* NHE) was more negative than the calculated minimum conduction band edge potential of Ag_3PO_4 (+0.27 eV *vs.* NHE), the production of $O_2^{\bullet-}$ radicals *via* the reduction of O_2 by CB electrons was difficult. According to the XRD results (Fig. 1b), the Ag^+ had been reduced by the photogenerated electrons ($E°(Ag^+/Ag)$ = + 0.80 eV *vs.* NHE) in Ag_3PO_4 suspension system *via* visible light irradiation. Silver nanoparticles are capable of storing electrons[28,29]. Therefore, the photogenerated electrons would transfer to Ag^0 nanoparticles and then reduce the present molecular oxygen to form the $O_2^{\bullet-}$ radicals active species[30]. In addition, due to the reduction potential of O_2 to H_2O_2 is higher than the potential of the conduction band in Ag_3PO_4, the transmission from the electrons in the CB of Ag_3PO_4 to oxygen species would be taken place through a multi-electron processes as shown[31] in eqns. 2, the reduced Ag^0 on the surface of Ag_3PO_4 particles promotes the multi-electron processes.

$$O_2 + 2H^+ + 2e^- \rightarrow H_2O_2;\ E_0 = +0.682\ eV \qquad (2)$$

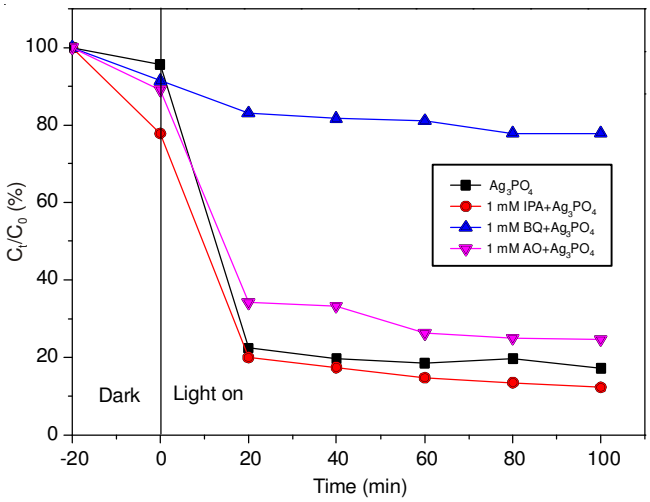

Fig. 8. Effect of the scavengers on the tetracyclines degradation rate

To further confirm the presence of •OH, the produced •OH on the surface of Ag_3PO_4 was detected by a photoluminescence (PL) technique using terephthalic acid as a probe. Fig. 9 shows the fluorescence spectral changes with the increasing time of visible light irradiation in the terephthalic acid solution (excitation wavelength at 315 nm). It can be seen the photoluminescence intensity around 425 nm significantly increased with the increasing of irradiation time and the strongest intensity achieved at 20 min, which indicated the hydroxyl radicals did produce. However, the photoluminescence intensity weakened laterly, suggesting the highly fluorescent product, 2-hydroxyterephthalic acid could be degradation in the Ag_3PO_4 suspension system. These results suggested that •OH radicals were the active oxygen species in the photocatalytic process. According the previous discussion, the photogenerated holes on the surface of Ag_3PO_4 could not react with H_2O to produce •OH, which was also consistant with the results of alkali condition experiments (Fig. 6). However, it was surprising that hydroxyl radicals were observed on the surface of Ag_3PO_4 with visible light irradiation through the fluorescence spectra. Therefore, it could be deduced that the conversion of •OH maybe carried out through other pathway rather than facile reaction between hole and H_2O. For example, H_2O_2 produced *via* a two-electron reduction reaction process as eqn. 2 at first and then the formed H_2O_2 quickly reacts with an electron to finally generate •OH, as shown[32] in eqn. (3):

$$H_2O_2 + e^- \rightarrow {}^{\bullet}OH + OH^- \quad (3)$$

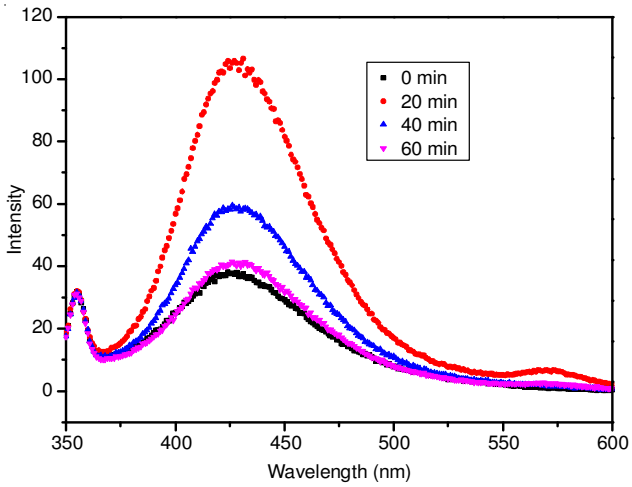

Fig. 9. •OH trapping photoluminescence spectral changes over Ag_3PO_4 in a 5×10^{-4} M terephthalic acid solution (excitation at 315 nm) with visible light irridiation time

Combining the above analysis, it was reasonable to hypothesize that the photocatalytic degradation of tetracyclines in the presence of Ag_3PO_4 was caused by the synergism effeciency of photogenerated holes, •OH and $O_2^{\bullet-}$.

On the base of the band gap structure of Ag_3PO_4 and the reactive oxygen species analysis results, a possible mechanism for the photodegradation of tetracyclines over Ag_3PO_4 photocatalyst under visible light irradiation was proposed (Fig. 10). Firstly, the as-prepared Ag_3PO_4 excited by the visible light illumination to produce the electron-hole pairs. The photogenerated holes remained in the valence band and then direcly oxidize the adsorbed tetracyclines molecules at the surface of Ag_3PO_4. On the other hand, the photogenerated electrons in the conduction band reduced a part of Ag^+ into metallic Ag at the initial stage which caused the form of Ag nanoparticles on the surface of Ag_3PO_4. The Ag nanoparticles could trap the following photoexcited electrons and inhibit the recombination of electrons and holes. Secondly, the trapped electron reacted with the O_2 to produce $O_2^{\bullet-}$ which photodegradated the tetracyclines molecules. At the same time, reactive •OH would also generate from H_2O_2 eqn. 3 caused by O_2 reacting with the trapped electron on Ag nanoparticles or the conduction band electrons *via* two-electron reduction process and then induced the mineralization of tetracyclines molecules. Thirdly, Ag nanoparticles formed on the surface of Ag_3PO_4 were beneficial for the separation of photogenerated electron-hole pairs and visible light absorption *via* surface plasmon resonance[24]. However, with the photocatalytic progress, the active sites on the surface of Ag_3PO_4 would be covered by the excessive amount of Ag nanoparticles which decreased the photocatalytic ability during the cycle experiments. Wang *et al.*[33] have further investigated the deactivation mechanism of Ag_3PO_4 spherical particles under visible-Light irradiation, they considered that Ag nanoparticles deposited on Ag_3PO_4 could prevent photogenerated electron-hole pairs from recombination by means of acting as electron trapping centers, but the shielding effect by Ag layers on the surface of Ag_3PO_4 would also decrease the photocatalytic activity. Therefore, it is not surprising that a part of decreasing in the photocatalytic activity of Ag_3PO_4 samples during the cycle experiments.

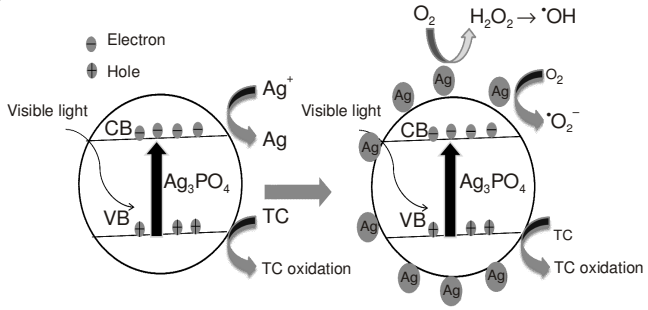

Fig. 10. Schematic diagram of the possible reaction mechanism over Ag_3PO_4 photocatalyst under visible light irradiation

Conclusion

The Ag_3PO_4 photocatalyst have been successfully synthesized *via* a simple solid phase ion-exchange method at room temperature. Under visible-light irradiation, as-prepared Ag_3PO_4 photocatalyst exhibited higher photocatalytic ability than BiOBr for tetracyclines degradation. On the basis of the reactive oxygen species trapping experiments results and mechanism analysis, $O_2^{\bullet-}$, •OH and h^+ were all reactive oxygen species in the visible light photocatalytic degradation tetracyclines process, the reduced metallic Ag particles played the important role in the form of $O_2^{\bullet-}$ and •OH radicals. The facile solid phase method, high visible light photocatalytic activity and favourable reusability of Ag_3PO_4 photocatalysts provided a potential approach toward the removal of antibiotics organic pollutants using sunlight.

ACKNOWLEDGEMENTS

The authors thank the National Natural Science Foundation of China (No. 21007010); Hu Nan Province Ministry of Transportation Scientific Research Project (No. 200908, 201105) and Ministry of Transport Science and Technology Program (No. 2010353343290).

REFERENCES

1. A. Fujishima and K. Honda, *Nature*, **238**, 37 (1972).
2. H. Tong, S.X. Ouyang, Y.P. Bi, N. Umezawa, M. Oshikiri and J. Ye, *J. Adv. Mater*., **24**, 229 (2012).
3. W. Jiang, J.A. Joens, D.D. Dionysiou and K.E. O'Shea, *J. Photochem. Photobiol. Chem*., **262**, 7 (2013).
4. P.H. Wang, P.S. Yap and T.T. Lim, *Appl. Catal. A*, **399**, 252 (2011).
5. G.P. Dai, J.G. Yu and G. Liu, *J. Phys. Chem. C*, **115**, 7339 (2011).
6. H.F. Cheng, B.B. Huang, Y. Dai, X.Y. Qin and X.Y. Zhang, *Langmuir*, **26**, 6618 (2010).
7. Z. Yi, J. Ye, N. Kikugawa, T. Kako, S. Ouyang, H. Stuart-Williams, H. Yang, J. Cao, W. Luo, Z. Li, Y. Liu and R.L. Withers, *Nat. Mater*., **9**, 559 (2010).
8. Y.P. Bi, S.X. Ouyang, N. Umezawa, J.Y. Cao and J.H. Ye, *J. Am. Chem. Soc*., **133**, 6490 (2011).
9. M. Ge, N. Zhu, Y. Zhao, J. Li and L. Liu, *Ind. Eng. Chem. Res*., **51**, 5167 (2012).
10. Z. Yi, J. Ye, N. Kikugawa, T. Kako, S. Ouyang, H. Stuart-Williams, H. Yang, J. Cao, W. Luo, Z. Li, Y. Liu and R.L. Withers, *Nat. Mater.*, **9**, 559 (2010).
11. X. Ma, B. Lu, D. Li, R. Shi, C. Pan and Y. Zhu, *J. Phys. Chem. C*, **115**, 4680 (2011).
12. H. Cheng, B. Huang, Y. Dai, X. Qin and X. Zhang, *Langmuir*, **26**, 6618 (2010).
13. Y.Y. Li, J.S. Wang, H.C. Yao, L.Y. Dang and Z.J. Li, *J. Mol. Catal. Chem*., **334**, 116 (2011).
14. J. Cao, B.D. Luo, H.L. Lin, B.Y. Xu and S.F. Chen, *J. Hazard. Mater*., **217-218**, 107 (2012).
15. C.T. Dinh, T. Nguyen, F. Kleitz and T. Do, *Chem. Commun.*, **47**, 7797 (2011).
16. A.H. Nethercot, *Phys. Rev. Lett*., **33**, 1088 (1974).
17. M.A. Butler, *J. Electrochem. Soc*., **125**, 228 (1978).
18. J. Jiang, X. Zhang, P.B. Sun and L.Z. Zhang, *J. Phys. Chem. C*, **115**, 20555 (2011).
19. J. Xu, W. Meng, Y. Zhang, L. Li and C.S. Guo, *Appl. Catal. B*, **107**, 355 (2011).
20. X.J. Shi, X. Chen, X.L. Chen, S.M. Zhou, S.Y. Lou, Y.Q. Wang and L. Yuan, *Chem. Eng. J*., **122**, 220 (2013).
21. Y. Wang, Z.Q. Shi, C.M. Fan, X.W. Wang, X.G. Hao and Y.Q. Chi, *J. Solid State Chem*., **199**, 224 (2013).
22. J. Li, W.H. Ma, Y.P. Huang, X. Tao, J.C. Zhao and Y.M. Xu, *Appl. Catal. B*, **48**, 17 (2004).
23. R. Palominos, J. Freer, M.A. Mondaca and H.D. Mansilla, *J. Photochem. Photobiol. Chem*., **193**, 139 (2008).
24. Y. Liu, L. Fang, H. Lu, Y. Li, C. Hu and H. Yu, *Appl. Catal. B*, **115-116**, 245 (2012).
25. X.D. Zhu, Y.J. Wang, R.J. Sun and D.M. Zhou, *Chemosphere*, **92**, 925 (2013).
26. J.F. Niu, S.Y. Ding, L.W. Zhang, J.B. Zhao and C.H. Feng, *Chemosphere*, **93**, 1 (2013).
27. W.Z. Yin, W.Z. Wang and S.M. Sun, *Catal. Commun*., **11**, 647 (2010).
28. A. Wood, M. Giersig and P. Mulvaney, *J. Phys. Chem. B*, **105**, 8810 (2001).
29. A. Takai and P.V. Kamat, *ACS Nano*, **5**, 7369 (2011).
30. J. Yu, G. Dai and B. Huang, *J. Phys. Chem. C*, **113**, 16394 (2009).
31. S.B. Rawal, S.D. Sung and W.I. Lee, *Catal. Commun*., **17**, 131 (2012).
32. X. Wang, M.T. Utsumi, Y.N. Yang, K. Shimizu, D.W. Li, Z.Y. Zhang and N. Sugiura, *Chem. Eng. J*., **230**, 172 (2013).
33. W.G. Wang, B. Cheng, J.G. Yu, G. Liu and W.H. Fan, *Chem. Asian J*., **7**, 1902 (2012).